Treatment for Expansive Soil Channel Slope with Soilbags

Sihong Liu[1]; Fuqing Bai[2]; Yisen Wang[3]; Shan Wang[4]; and Zhuo Li[5]

Abstract: Expansive soil is regarded as one of the trouble soils and is difficult to deal with in engineering because of its strong swelling–shrinkage behavior and well-developed fissures and overconsolidation. In this paper, a treatment method for an expansive soil channel slope with soilbags is proposed. The mechanism of the proposed treatment method is introduced. A number of the swell potential, swelling pressure, seepage, and interlayer friction tests were conducted on soilbags filled with expansive soils, which were taken from a construction site of the South-to-North Water Transfer Project in China. The test results indicate that soilbags can enhance the strength and restrict the swelling deformation of the expansive soil, and that the assembly of soilbags has a high permeability and interlayer friction coefficient. The stability of an expansive channel slope reinforced by soilbags is analyzed based on the limit-equilibrium theory. **DOI: 10.1061/(ASCE)AS.1943-5525.0000198.**

CE Database subject headings: Expansive soils; Friction; Soil permeability; Swelling (material); Soil deformation; Slope stability; China.

Author keywords: Expansive soil; Interlayer friction; Permeability; Soilbag; Swelling deformation; Stabilization.

Introduction

Expansive soils have characteristics of high plastic limits, developed cracks, strong swelling and shrinkage, and strength retrogression, originating from the components of montmorillonite and other clay minerals. Expansive soils occur in many parts of the world, but particularly in arid and semiarid regions (Chen 1988). In these regions, evaporation rates are higher than the average annual rainfall so that there is almost always a moisture deficiency in the soil and the soil is in an unsaturated state. In a rainy or wet season, volume expansion of expansive soils occurs owing to water absorption; on the other hand, in a dry season, expansive soils exhibit shrinkage because of water loss, causing soil cracking (Chen 1988; Lu and Likos 2004). The engineering problems associated with unsaturated expansive soils extend over an enormous range, including foundations, retaining walls, pavements, canal beds, and slope stability.

There are many factors that govern the behaviors of an expansive soil, among which the primary ones are the availability of moisture and the amount and type of the clay-size particles in the soil (Day 2000). Therefore, the treatment methods for expansive soils may be classified into two categories: one is to use the so-called chemical and mechanical stabilization method, and the other is to retard moisture movement within the soil. The mechanical stabilization may include the preloading method, the sand cushion method (Satyanarayana 1966), the cohesive nonswelling (CNS) layer method (Katti 1979), and the synthetic reinforcement method. In the chemical treatment method, lime is the most effective and economical added material (Chen 1988). Otherwise, calcium chloride and fly ash are also commonly used (Desai and Oza 1997; Sharma et al. 2008). The retardation of moisture movement within expansive soils may be achieved by the coverage with geomembrane.

Now, in China, the South-to-North Water Transfer Project (SNWTP) with three diversion routes (named the eastern, the central, and the western lines, respectively) is under construction. The central diversion route is 1,200 km long, of which approximately 180 km of open channel has to pass through land with expansive soil (Ng et al. 2003). Hence, the stability of the expansive soil channel slope is particularly important for the project. The basic way to stabilize the expansive soil channel slope is to replace the expansive soils near the surface of the channel slope (approximately 2 m thick) with nonexpansive soils. Because nonexpansive soils have to be taken from areas far away from the construction site, this method of soil replacement is expensive and has some expropriation and environmental problems. Therefore, alternative ways of treating expansive soil slope have to be studied. In recent years, extensive studies have been made, and many other methods have been proposed for the treatment of the expansive soil slope, one of which is the use of soilbags filled with expansive soils.

Fig. 1 shows the schematic view of the treatment using soilbags. The expansive soils excavated in the construction field are filled into woven polypropylene bags to form soilbags, which are then arranged on the surface of the expansive soil slope to be treated. The assembly of soilbags arranged on the slope is regarded as a reinforcement layer and has the effect of restraining the expansion and contraction of expansive soils.

Soilbags have long been used in embankment-raising at times of inundation and as temporary structures during reconstruction after disasters. In recent years, with the reinforcement principle of soilbags being elucidated, soilbags have gradually been used in permanent or semipermanent civil works and verified to be feasible and effective [E. Khalili, "Earthquake resistant building structure employing sandbags," U.S. Patent No. 5,934,027 (1999); Matsuoka and Liu 2003; Nakagawa et al. 2008; Tatsuoka and Tateyama 1997].

[1]Professor, Research Institute of Hydraulic Structures, Hohai Univ., Nanjing 210098, China. E-mail: sihongliu@hhu.edu.cn

[2]Research Associate, Research Institute of Hydraulic Structures, Hohai Univ., Nanjing 210098, China (corresponding author). E-mail: baifuqing@163.com

[3]Professor, Experts' Committee of the South-to-North Water Diversion Project Commission of the State Council, Beijing 100142, China. E-mail: wang_ys@sina.com

[4]Research Associate, Research Institute of Hydraulic Structures, Hohai Univ., Nanjing 210098, China. E-mail: cowangshan1130@126.com

[5]Research Associate, Research Institute of Hydraulic Structures, Hohai Univ., Nanjing 210098, China. E-mail: slxliz@163.com

Note. This manuscript was submitted on March 2, 2011; approved on January 9, 2012; published online on January 11, 2012. Discussion period open until March 1, 2014; separate discussions must be submitted for individual papers. This paper is part of the ***Journal of Aerospace Engineering***, Vol. 26, No. 4, October 1, 2013. ©ASCE, ISSN 0893-1321/2013/4-657–666/$25.00.

A new earth-reinforcement method using soilbags has been developed(Matsuoka and Liu 2003; Matsuoka and Liu 2005). However, the soilbag method has not yet been applied to stabilize expansive soil slope.

In this paper, the principle of reinforcing expansive soils using soilbags is first introduced. A series of laboratory experiments is then carried out on soilbags filled with expansive soils to study the physical and mechanical properties of the swelling deformation, the permeability, and the friction between soilbag layers. Based on the rigid limit-equilibrium theory, a method of analyzing the slope stability reinforced with soilbags is proposed.

Principle of Reinforcing Expansive Soil with Soilbag

In this paper, the soilbag filled with expansive soils is referred to as expansive soilbag. Fig. 2 illustrates the reinforcement principle of an expansive soilbag. The reinforcement of a soilbag is mainly attributed to the tensile force T along the bag, which is developed owing to the extension of the bag perimeter. For an expansive soilbag, the extension of the bag perimeter is caused not only by the action of external forces, but also by the swelling deformation of expansive soils during the wetting process. The tensile force T along the bag enhances the contacts between the soil particles inside the bag, resulting in the increase in the normal contact force N and the frictional force F between soil particles ($F = \mu N$, where μ is the friction coefficient). Therefore, the expansive soilbag behaves with high strength. By the way, the consolidation or evaporation would lead to the volume shrinking of an expansive soil. In this case, the tensile stress in the soilbag is only induced by the external forces applied.

Matsuoka and Liu (2003) derived a strength formula for a two-dimensional model soilbag based on the Mohr-Coulomb theory. In this paper, the soilbag is regarded as a three-dimensional (3D) cuboid, and its strength is reconsidered. Fig. 3 illustrates the stress states of a cuboid soilbag and a soil element inside the bag. Under the actions of the three major principal stresses σ_{1f}, σ_{2f}, and σ_{3f} (subscript f denotes the state at failure) and the swelling of the expansive soils inside the bag, the expansive soilbag becomes flatter generally and deforms laterally. Consequently, a tensile force T is developed along the bag, which produces an additional stress on the particles inside the bag with the components of σ_{1b}, σ_{2b}, and σ_{3b}, respectively. As illustrated in Fig. 3(a), the force equilibrium in the B–L section plane of the soilbag gives the additional stress component, σ_{1b}:

$$\sigma_{1b} = \frac{T \times (2B) + T \times (2L)}{B \times L} = \frac{2T}{L} + \frac{2T}{B} \tag{1a}$$

Similarly, the additional stress components of σ_{2b} and σ_{3b} are as follows:

$$\sigma_{2b} = \frac{T \times (2H) + T \times (2B)}{H \times B} = \frac{2T}{B} + \frac{2T}{H} \tag{1b}$$

$$\sigma_{3b} = \frac{T \times (2L) + T \times (2H)}{L \times H} = \frac{2T}{H} + \frac{2T}{L} \tag{1c}$$

where L, B, and H = length, width, and height of the soilbag, respectively. As illustrated in Fig. 3(b), the stresses acting on the soil element inside the bag are thus the combination of the external stresses and the additional stress caused by the tensile force T. At failure, based on the Mohr-Coulomb theory, the major principle stress σ_{1f} can be calculated by

$$\sigma_{1f} = \sigma_{3f} \cdot \frac{1+\sin\phi}{1-\sin\phi} + 2T\left(\frac{1}{H}+\frac{1}{L}\right)\frac{1+\sin\phi}{1-\sin\phi} - 2T\left(\frac{1}{L}+\frac{1}{B}\right) + \frac{2c\cdot\cos\phi}{1-\sin\phi} \tag{2}$$

Assuming $K_p = (1+\sin\phi)/(1-\sin\phi)$, Eq. (2) is rewritten as

$$\sigma_{1f} = \sigma_{3f}K_p + 2T\left(\frac{1}{H}+\frac{1}{L}\right)K_p - 2T\left(\frac{1}{L}+\frac{1}{B}\right) + 2c\sqrt{K_p} \tag{3}$$

in which K_p = lateral earth-pressure ratio at passive state; and c and ϕ = cohesion and friction angle of expansive soil inside the bag, respectively. Assuming that the internal friction angle of the soilbag is the same as that of the soil filling the bag, the total cohesion of the soilbag c_{total} is thereby expressed as

$$c_{\text{total}} = c + \frac{T}{\sqrt{K_p}}\left[\left(\frac{1}{H}+\frac{1}{L}\right)K_p - \left(\frac{1}{L}+\frac{1}{B}\right)\right] = c + c_T \tag{4}$$

Eq. (4) illustrates that the total cohesion c_{total} of the soilbag consists of two parts: one is the inherent cohesion c of the expansive soil, and the other is the additional cohesion c_T caused by tensile force T of the bag. The latter depends on the dimension of the soilbag, the tensile force of the bag, and the friction angle of the soil filling the bag.

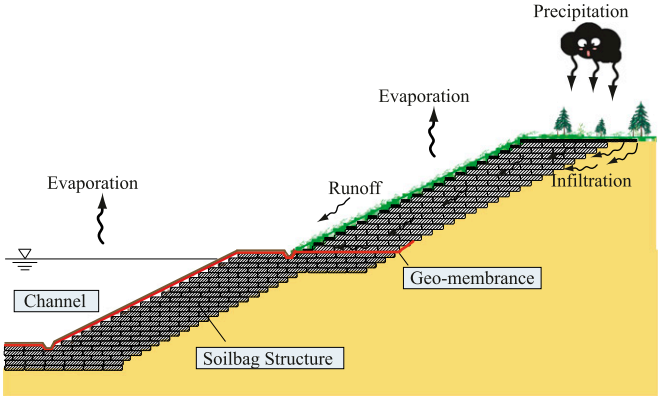

Fig. 1. Illustration of stabilizing expansive soil slope with soilbags

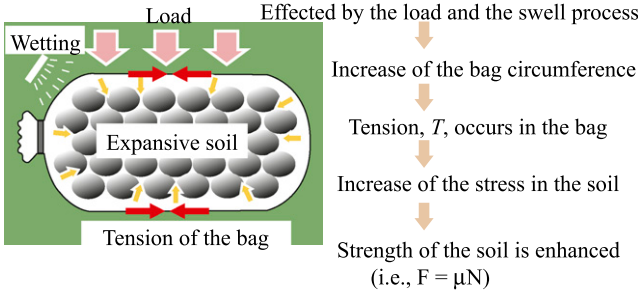

Fig. 2. Principle of reinforcing expansive soil with soilbags

Swelling Characteristics of Expansive Soilbags

To verify the effectiveness of the proposed soilbag method, the swelling potential under overburdens and the swelling pressures for soilbags filled with a typical Nanyang (NY) expansive soil are

J. Aerosp. Eng. 2013.26:657-666.

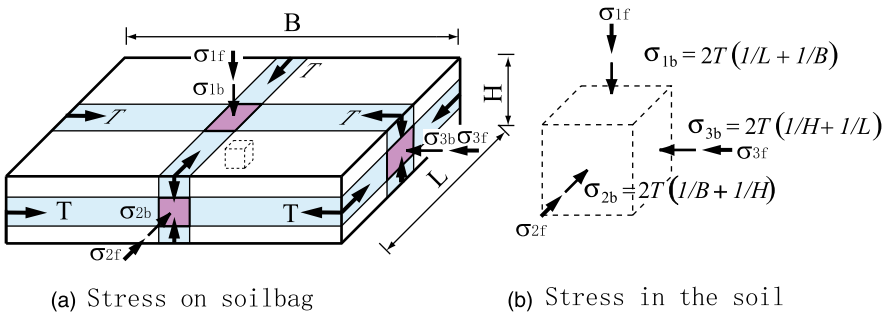

(a) Stress on soilbag (b) Stress in the soil

Fig. 3. Force analysis of soilbag in 3D stress state

investigated, and the strength properties of the expansive soilbags are discussed.

Expansive Soilbags

The expansive soil used in this study was obtained from a construction field of the South-to-North Water Transfer Project in Nanyang, China. It is a kind of Quaternary–Miocene alluvial–pluvial clay (Bao and Ng 2000), mainly containing the mineral components of montmorillonite and illite, with contents of approximately 40 and 9%, respectively. The expansive soil has a maximum dry density of 1.76 g/cm^3 and an optimum water content of 20.4%, determined as per Chinese soil-testing standard SL237-1999 (Ministry of Water Resources 1999). The liquid limit and the plastic limit of the soil are 60.2 and 30.2%, respectively. The free swelling ratio (FSR) of the soil is approximately 119.5%. The grain-size distribution of the soil is presented in Fig. 4.

The bag used to contain the expansive soil is a kind of woven geotextile made of polypropylene and has a size of 57 × 45 cm (warp length × weft width). The tensile tests were conducted on bag strips with a length of 10 cm and a width of 5 cm. The measured tensile forces per unit width both in warp and weft directions are plotted against strains in Fig. 5. It is shown that the tensile force per unit width of the bag increases approximately linearly with the increasing strain, having a tensile modulus of 1.61 and 1.38 kN/m in warp and weft directions, respectively. The average tensile strengths, the maximum force per unit width to cause a specimen to rupture, are approximately 25 and 16 kN/m in warp and weft directions, respectively.

To make a soilbag, the expansive soil was first air dried and crushed to pass through a 2-cm sieve. It was then mixed with a required amount of distilled water to obtain two different water contents of 20 and 24%. Upon equilibrium in a sealed container by 24 h, the soil was filled into the woven geotextile bags, and the bags were then sealed and compacted to a dry density of 1.6 g/cm^3 for the swell overburden test and 1.5 g/cm^3 for the swell pressure test. The prepared soilbag is approximately 43 cm in length, 41 cm in width, and 6.5 cm in height.

Swell Potential of Expansive Soilbag under Overburdens

The swell potential of an expansive soil under vertical loads (overburdens) is investigated through the swell overburden test. In a conventional swell overburden test (CSOT), the expansive soil is placed in an oedometer and inundated under a constant vertical pressure until the vertical swelling deformation of the soil specimen is less than 0.01 mm/h. In a similar way to the CSOT, a simplified swell overburden test (SSOT) was designed for measuring the overburden swell potential of an expansive soilbag, as illustrated in

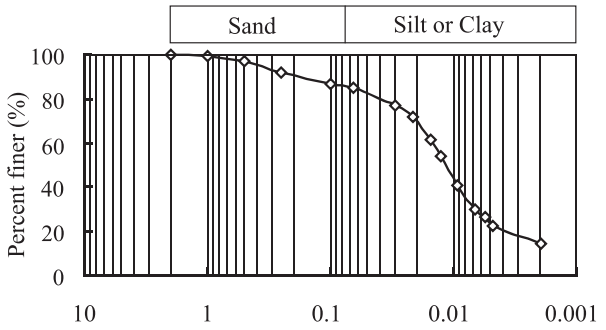

Fig. 4. Grain-size distribution of NY unsaturated expansive soil

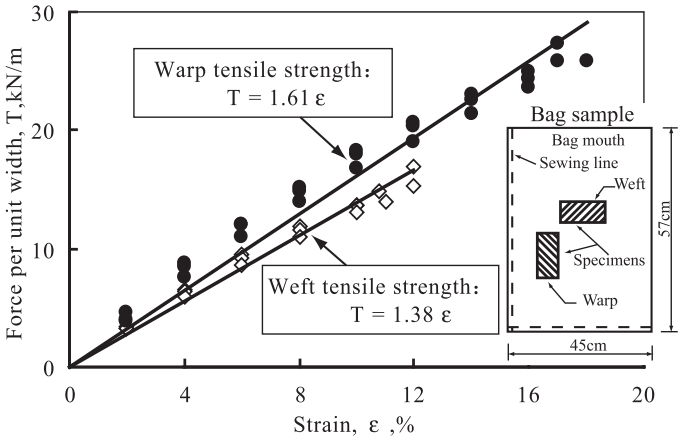

Fig. 5. Tensile strength of bag

Fig. 6. In the SSOT, an expansive soilbag is placed between two porous plane supports on a reaction frame. To minimize the friction effect, the soilbag and the plane supports are separated from each other with a piece of woven geotextile. Two dial indicators are set diagonally on the top support to measure the vertical displacement of the soilbag tested. The lateral deformation of the soilbag is measured with dial indicators located at the sides of the soilbag. A constant vertical pressure is applied on the soilbag specimen using an oil jack. Under this constant vertical pressure, the soilbag specimen is wetted by injecting water from the two porous plane supports continuously until the vertical swelling deformation of the soilbag is less than 0.01 mm/hour.

The SSOTs have been performed on two groups of the expansive soilbags with the same initial dry density but different initial water contents. In Group A, four expansive soilbags with an initial water

J. Aerosp. Eng. 2013.26:657-666.

content of 20% are prepared, and the vertical (overburden) pressures of 15.5, 30, 50, and 100 kPa, respectively, are applied on each of the expansive soilbags to investigate the effect of the overburden pressure on the swell potential of the soilbags. In Group B, three expansive soilbags with an initial water content of 24% are prepared, and the vertical pressures of 15.5, 40, and 50 kPa, respectively, are applied on each soilbag. Meanwhile, the CSOTs are comparatively performed on the expansive soil under the same initial conditions as the SSOTs on the soilbags.

Fig. 7 gives the comparison of the vertical and volumetric swell of both the expansive soil and the soilbags under different pressures applied. In this paper, the vertical swell is defined as the ratio of the increase in the specimen height to the original one; the volumetric swell is the ratio of the increase in the specimen volume to the original one. It is shown that the swell of the soilbag is smaller than that of the expansive soil inside the soilbag at the same overburden pressure. The effectiveness of soilbags to restrict the swell of expansive soils is thus illustrated. The results in Fig. 7 also indicate the effect of overburden loading to restrict swell. The swell of both the expansive soil and the soilbags decreases significantly under lower overburden pressures and almost tends to a constant when the overburden pressure applied is larger than 40 kPa.

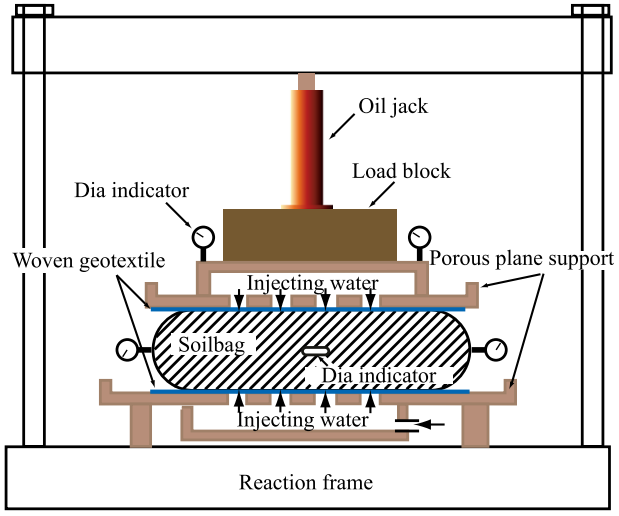

Fig. 6. Illustration of swell overburden test on expansive soilbag

The circumference increments of the soilbags during the SSOT can be calculated approximately with the measured vertical and lateral displacements. Figs. 8 and 9 show the development of the circumference increments of the soilbags in Group A and in Group B, respectively, the maximum values of which are listed in Table 1. It is shown that there is a similar development of the circumference increments of the soilbags in the warp and in the weft during the SSOTs.

As previously discussed, the tensile force in an expansive soilbag is attributable to both the compaction and the swell. The total tensile force T is thus

$$T = E(\Delta\varepsilon_1 + \Delta\varepsilon_2) \tag{5}$$

where E = tensile modulus of the bag (i.e., 1.61 kN/m in the warp and 1.38 kN/m in the weft); $\Delta\varepsilon_1$ = strain increment produced during the compaction, calculated from the size change of the soilbag; and $\Delta\varepsilon_2$ = swell-strain increment produced during the SSOT.

For the expansive soilbag tested, the circumference of the soilbag before the compaction is 942 mm in the warp and 900 mm in the weft; after the compaction, it becomes 990 mm in the warp and 950 mm in the weft. Thus, $\Delta\varepsilon_1$ is 5.1% in the warp and 5.8% in the weft, which produces a tensile force of 8.2 kN/m in the warp and 8.0 kN/m in the weft. The swell-induced tensile forces corresponding to $\Delta\varepsilon_2$ and the total tensile forces of the expansive soilbags are presented in Table 1. It is shown that the total tensile force in the warp is closely equal to the one in the weft for each soilbag tested. Thereby, the apparent cohesion of a soilbag can be calculated from either the tensile force in the warp or that in the weft.

From Eq. (4), the apparent cohesion, c_T, of the soilbag can be calculated as

$$c_T = \frac{T}{\sqrt{K_p}}\left[\left(\frac{1}{B}+\frac{1}{H}\right)K_p - \left(\frac{1}{L}+\frac{1}{B}\right)\right] \tag{6}$$

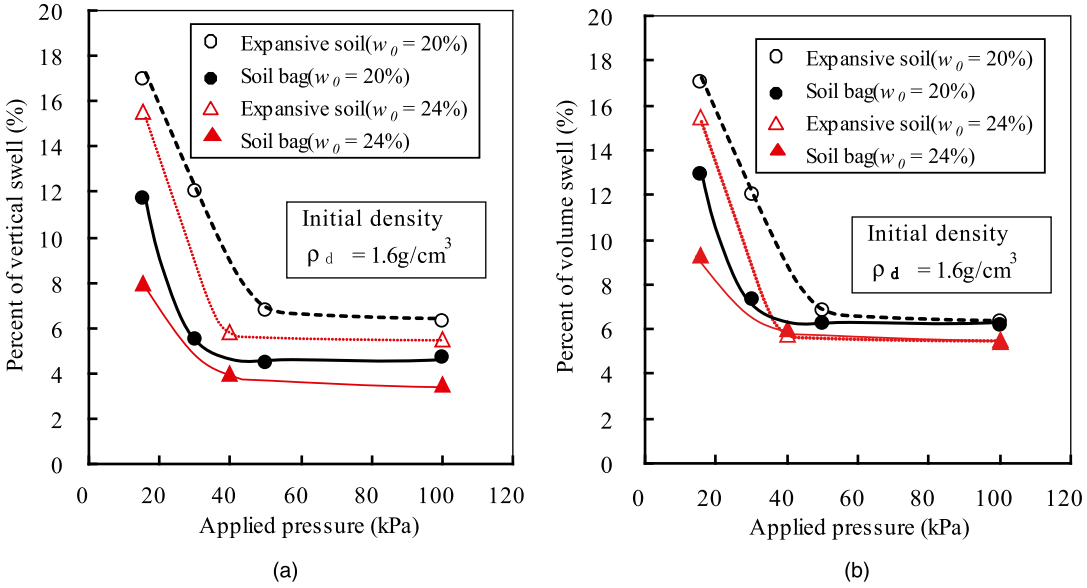

Fig. 7. Comparison of swell potential of expansive soil and soilbags under different pressures applied: (a) vertical swell; (b) volume swell

J. Aerosp. Eng. 2013.26:657-666.

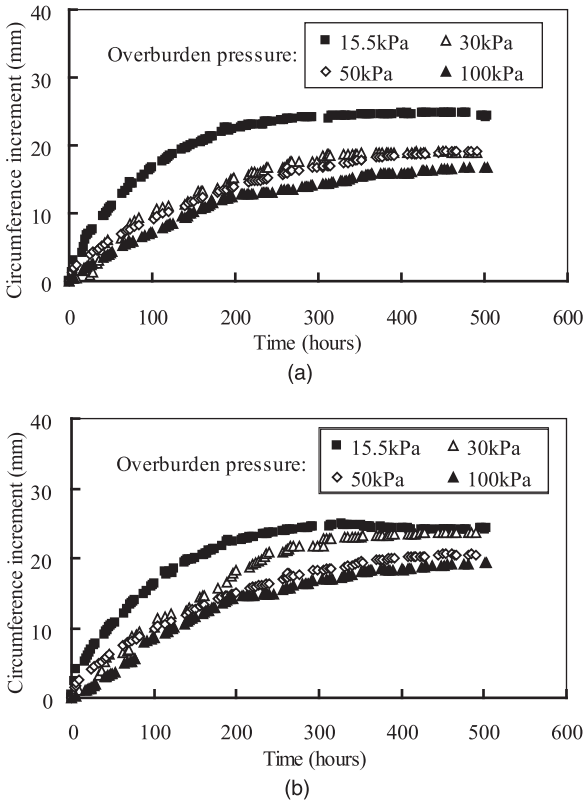

Fig. 8. Circumference increments of expansive soilbags in Group A during SSOTs: (a) warp increment; (b) weft increment

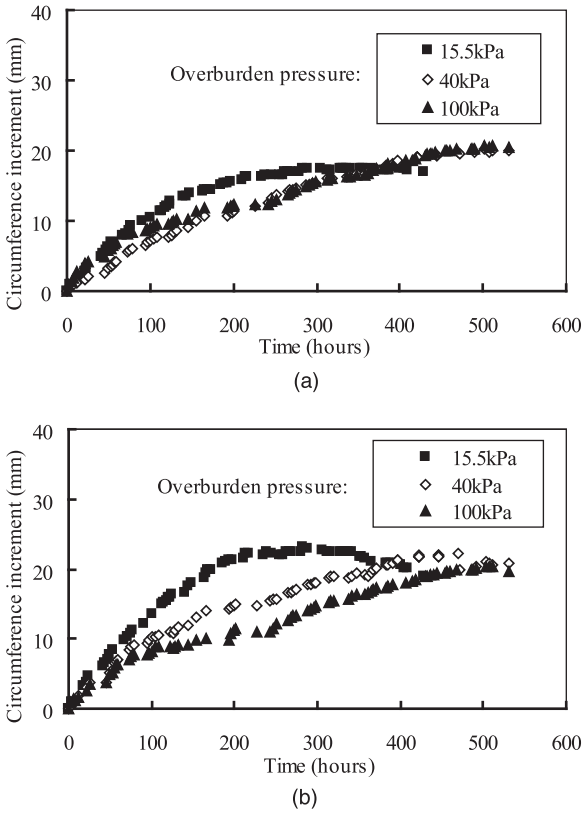

Fig. 9. Circumference increments of expansive soilbags in Group B during SSOTs: (a) warp increment; (b) weft increment

in the warp direction, and

$$c_T = \frac{T}{\sqrt{K_p}}\left[\left(\frac{1}{H}+\frac{1}{L}\right)K_p - \left(\frac{1}{L}+\frac{1}{B}\right)\right] \tag{7}$$

in the weft direction. The friction angle ϕ and the cohesion c of the unsaturated expansive soil filling the soilbag are approximately 12° and 126 kPa, respectively. The apparent cohesions of the expansive soilbags calculated using Eqs. (6) and (7) are presented in Table 1 and are close to 200 kPa and much higher than that of the expansive soil filling the soilbag.

Swelling Pressures of Expansive Soil and Soilbag

The constant volume test (CVT) is used to evaluate the swelling pressure of an expansive soil. In a CVT, the soil specimen is placed in an oedometer, and its vertical expansion when flooded with water is prevented by applying small, convenient vertical load increments. The swelling pressure is defined as the sum of the load increments throughout the swelling process divided by the cross-sectional area of the specimen (Al-Mhaidib 1998). In a similar way as the CVT, the swelling pressure of an expansive soilbag is tested using the setup as shown in Fig. 6 under the constant height of the soilbag specimen when inundated with water, which is achieved by applying small vertical load increments.

In this study, the swelling pressures of the expansive soil with an initial water content of 20% under different initial densities were measured in the CVTs, which are plotted against the initial densities in Fig. 10(a). It is shown that the swelling pressure of the expansive soil tested decreases rapidly as the initial density decreases.

The swelling pressure of the expansive soilbag with the initial water content of 20% and the initial density of 1.5 g/cm^3 is shown in Fig. 10(b). The measured swelling pressure of the soilbag is approximately 66.1 kPa, which is much smaller than that of the expansive soil at the same initial conditions (approximately 361.0 kPa). The difference is mainly attributable to the nonrigid constraint and possible deformation of the soilbag in the lateral direction. As a result, the volume of the soilbag increases and the density of the expansive soil filling the bag decreases, although the vertical deformation of the soilbag is not allowed. The expansive soilbag tested deforms from an initial size of $47.3 \times 40.7 \times 7.3$ cm (length $\times$ width $\times$ height) to a size of $48.1 \times 44.74 \times 7.3$ cm with density of 1.34 g/cm^3 after swelling. So, the measured swelling pressure of the expansive soilbag is close to that of the expansive soil at the density of 1.34 g/cm^3, as shown in Fig. 10(b).

Permeability of Soilbag Assembly

The permeability of the assembly of the soilbags arranged on the channel slope is very important because it affects highly the change of the moisture content not only in the reinforcement layer but also in the underlying expansive soil. To evaluate the permeability of the assembly of the soilbags, a large-scale permeability test was carried out in a specially designed transparent water tank with dimensions of $160 \times 100 \times 80$ cm (length $\times$ width $\times$ height).

Fig. 11 shows the permeability test on an assembly of the expansive soilbags under a constant water head both in the vertical and horizontal directions. Twenty expansive soilbags with an initial water content of 20% and a density of 1.6 g/cm^3 were prepared in advance on the ground. One has a size of $40 \times 40 \times 12$ cm

J. Aerosp. Eng. 2013.26:657-666.

Table 1. Results of SSOTs on Expansive Soilbags

Group	Initial water content (percentage)	Vertical pressure applied (kPa)	ΔC_{wp} (mm)	ΔST_{wp} (kN/m)	T_{wp} (kN/m)	c_{Twp} (kPa)	ΔC_{wt} (mm)	ΔST_{wt} (kN/m)	T_{wt} (kN/m)	c_{Twt} (kPa)
A	20	15.5	24.7	4.2	12.4	225.0	24.2	3.7	11.7	210.7
		30	24.2	3.7	11.7	210.7	24.2	3.7	11.7	210.7
		50	23.5	3.6	11.6	208.9	23.5	3.6	11.6	208.9
		100	16.8	2.9	11.1	201.4	19.3	3.0	11.0	198.1
B	24	15.5	17.4	3.0	11.2	203.3	23.2	3.5	11.5	207.1
		40	20.3	3.5	11.7	212.3	22.3	3.4	11.4	205.3
		100	20.7	3.5	11.7	212.3	20.4	3.1	11.1	199.9

Note: ΔC_{wp} and ΔC_{wt} = swell-induced circumference increment in warp and weft directions, respectively; ΔST_{wp} and ΔST_{wt} = swell-induced tensile force in warp and weft directions, respectively; T_{wp} and T_{wt} = total tensile force and swell-induced tensile force in warp and weft directions, respectively; and c_{Twp} and c_{Twt} = apparent cohesion of expansive soilbag in warp and weft directions, respectively.

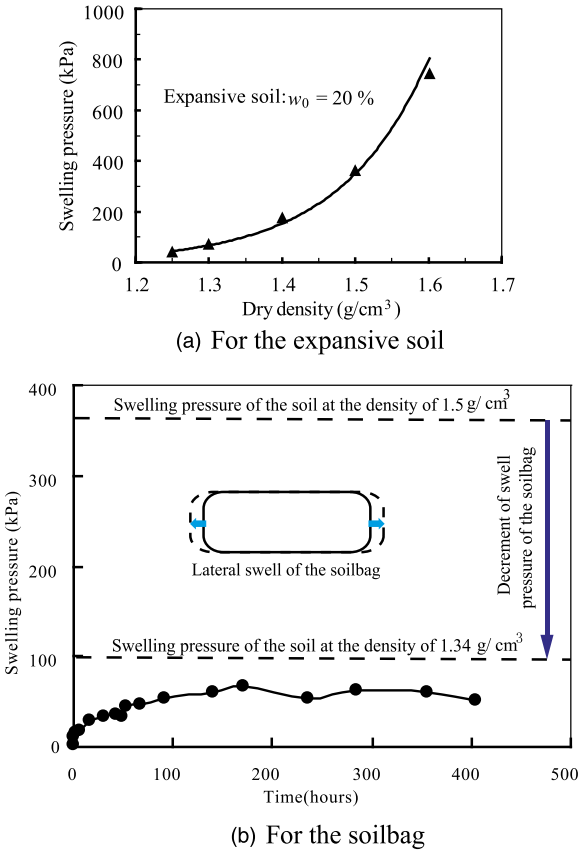

Fig. 10. Swelling pressure of soilbag and expansive soil inside bag: (a) expansive soil; (b) soilbag

(length × width × height). The assembly of soilbags consists of five layers: four soilbags for each layer, with the gaps between the soilbags filled with the same expansive soils as in the bags. A rigid top cap was placed on the soilbag assembly and then fixed with several bolts onto the side walls of the apparatus to keep a constant volume of the specimen during the test. Each specimen of the soilbag assembly was saturated in the water-filled tank for approximately 5 h before testing.

The permeability tests were performed under two constant water heads of 1.0 and 1.5 m, respectively. For the vertical seepage, an inlet is set on the capping of the vent, and water percolates through the soilbag specimen downward; for the horizontal seepage, the water head is applied laterally—i.e., water flows through the soilbag specimen from the left sealed water flume to the right unsealed water flume. After the tests, the gravimetric water content of the soil filling the bags was measured to be roughly 27%, approximately the value of the identically compacted soil specimen saturated under the vacuum condition. Meanwhile, the permeability of the saturated expansive soil inside the bags has also been tested using the falling water head method [SL237–1999 (Ministry of Water Resources 1999)].

Table 2 presents the permeability coefficients of the assembly of the soilbags and the expansive soil filling the bags. The measured permeability coefficient is approximately 10^{-5} to 10^{-6} m/s for the soilbag assembly and 10^{-8} m/s for the saturated expansive soil. The latter is in accordance with the field test results as reported by Zhan et al. (2007). From Table 2, it is shown that the horizontal permeability coefficient of the soilbag assembly is nearly 10 times higher than the vertical one. The high permeability of the soilbag assembly is attributable to the existence of gaps and contact surfaces between soilbags. The vertical seepage mainly flows through the gaps, whereas the horizontal seepage mainly flows through the contact surfaces. Thus, the soilbag assembly can be regarded as a semipermeable material, and any water penetrating into the assembly of the soilbags may drain away quickly.

As illustrated in Fig. 1, the proposed treatment method is to replace the extensively active zone of the expansive soils with an assembly of soilbags. The test results in Table 2 indicate that it is possible to minimize the variation of the water contents not only in the reinforced layer but also in the underlying expansive soils, probably caused by the rainfall or the change of the underground water. This feature is very important in the treatment of expansive soils.

Friction between Expansive Soilbags

The friction between soilbags affects greatly the stability of the assembly of soilbags on a slope. In this study, a number of pulling tests have been carried out on the soilbags with different arrangements. Because the soilbag is relatively flexible, the soilbags in an upper layer can cross the gaps between soilbags in the lower layer with close contact under the application of a vertical load, which is called the interlocking effect in this paper. Hence, the friction between soilbags consists of two components: one is the flat friction of the polypropylene bags, and the other is the interlocking effect that depends on the gaps between the soilbag layers. As shown in Fig. 12(a), the soilbags may contact on two different types of the gap: (1) the upper soilbag is placed on the gap formed between two soilbags (denoted as Type A); and (2) the upper soilbag is placed on the gap formed by four soilbags (denoted as Type B). In Fig. 12(a), A_i and B_i denote the pulling tests on the soilbags with these two types of gaps, respectively, where i is the number of the gaps. The expansive soil filling the tested soilbags has a water content of 20% and a dry density of 1.6 g/cm^3.

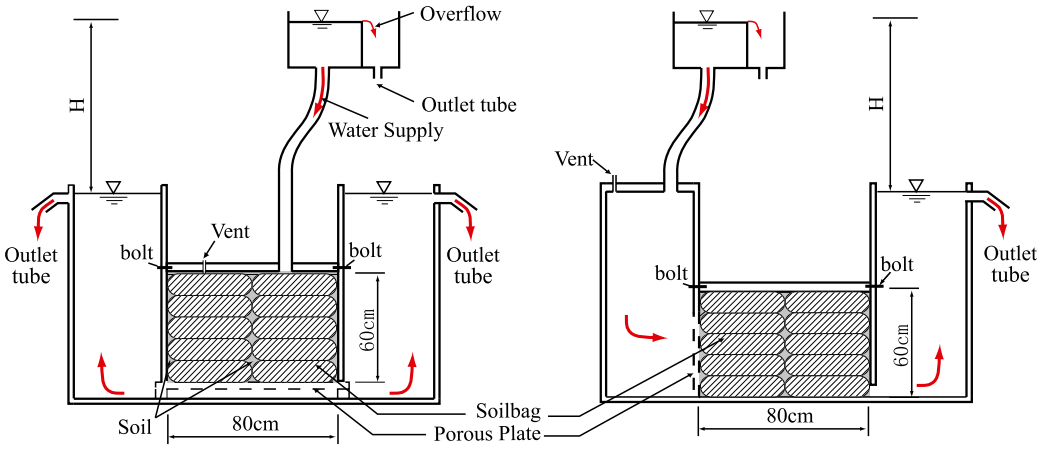

Fig. 11. Permeability test on assembly of expansive soilbags

Table 2. Permeability Coefficients of Assembly of Soilbags and Soils inside Bags

Specimen type	Water head (m)	Value of k_y			Value of k_x		
		First	Second	Average	First	Second	Average
Assembly of soilbags	1.0	5.7×10^{-6}	7.3×10^{-6}	6.5×10^{-6}	3.9×10^{-5}	3.6×10^{-5}	3.8×10^{-5}
	1.5	5.2×10^{-6}	6.5×10^{-6}	5.8×10^{-6}	3.2×10^{-5}	2.8×10^{-5}	3.0×10^{-5}
Expansive soil inside bag	Falling water head	1.6×10^{-8}	1.2×10^{-8}	1.4×10^{-8}	—	—	—

Note: k_x and k_y = permeability coefficients in horizontal and vertical directions.

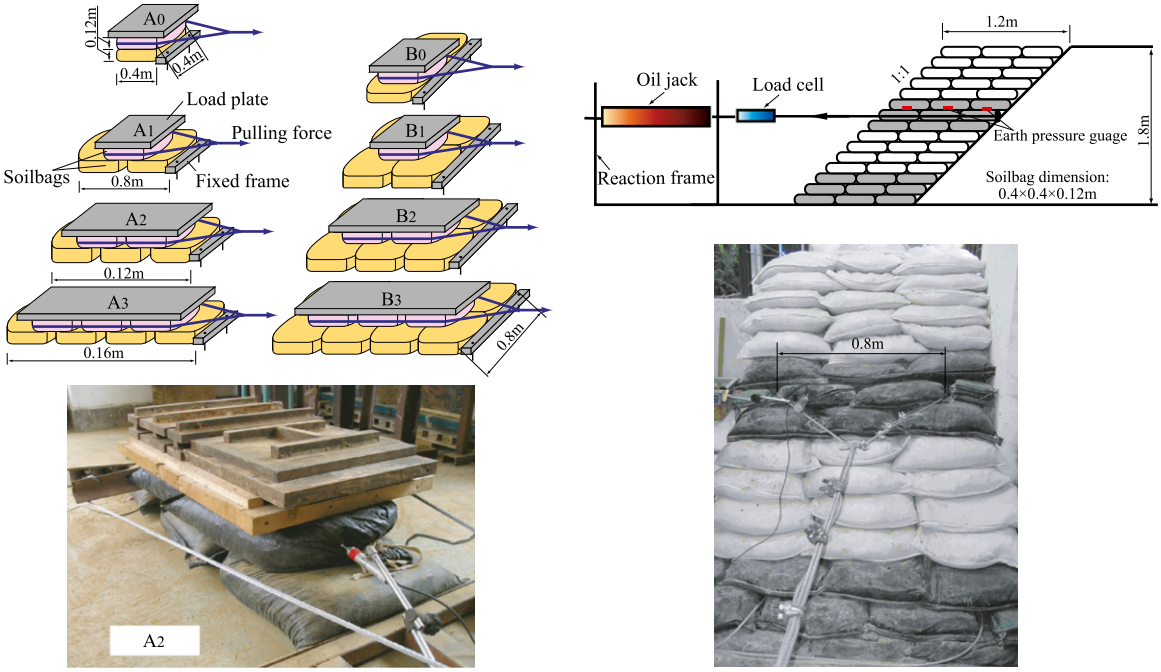

(a) Different arrangements

(b) Model slope of soilbags

Fig. 12. Pulling tests on assemblies of soilbags: (a) different arrangements; (b) model slope of soilbags

In the study, the pulling test has also been conducted on a model slope piled up with three rows of soilbags as shown in Fig. 12(b). The model slope is 1.5 m high and has a gradient of 1:1. A layer of soilbags was pulled by an oil jack, and the pulling force was measured with a load cell connected with the oil jack. To measure the overburden stress acting on the tested soilbags in the model slope, three earth-pressure gauges were placed on the top surface of the soilbags tested.

Fig. 13 presents the evolution of the pulling forces measured in the tests of A_0, A_1, B_0, and B_1 under a constant vertical load of 1,468 N. In the test A_0, the pulling force increases rapidly and tends to a constant after the sliding between the surfaces of the two soilbags.

J. Aerosp. Eng. 2013.26:657-666.

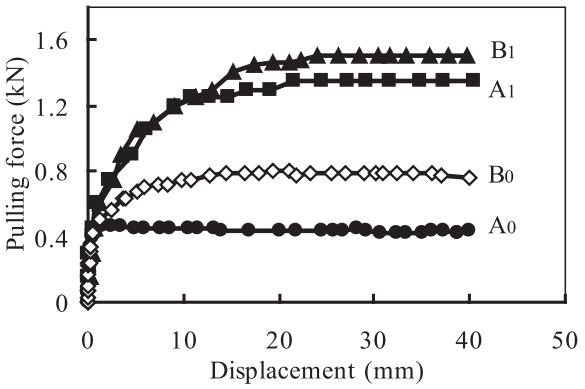

Fig. 13. Evolution of pulling forces in tests of A_0, B_0, A_1, and B_1

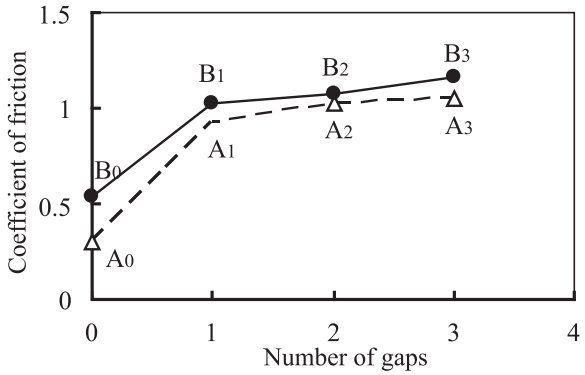

Fig. 14. Increase of equivalent coefficients of friction of soilbag assembly with number of interlayer gaps

Table 3. Equivalent Friction Coefficients between Soilbags Measured by Pulling Tests

Tests	Number of upper soilbags (number of lower soilbags)	Vertically applied force (N)	Pulling force after slip between soilbags (N)	Equivalent coefficient of friction between soilbags
A_0	1 (1)	1,468	435	0.30
A_1	1 (2)	1,468	1,362	0.92
A_2	2 (3)	1,668	1,700	1.02
A_3	3 (4)	1,195	1,250	1.05
B_0	1 (1)	1,468	787	0.54
B_1	1 (4)	1,468	1,495	1.02
B_2	1 (6)	2,428	2,623	1.08
B_3	3/8	1,675	1,950	1.16

In the tests of B_0, B_1, and A_1, the pulling forces increase gently because the upper soilbag has to stride over the gap in the lower soilbags. In this paper, the friction between soilbags is represented with an equivalent coefficient of friction, which is defined as the ratio of the peak pulling force measured in the pulling test to the vertically applied force. Table 3 gives the summary of the equivalent coefficients of friction between the soilbags measured in the pulling tests. Fig. 14 shows the increase of the equivalent coefficients of friction of the soilbag assembly with the number of interlayer gaps. It is shown that the soilbag assembly on Type B gaps has a higher friction than on Type A gaps, and the equivalent friction coefficient of the soilbag assembly with interlayer gaps is larger than 0.9.

Fig. 15 shows the evolution of the pulling force measured during the test on the model slope of soilbags. The overburden load acting on the tested soilbags is approximately 5,540 N, which is the product of the measured overburden stress by the total area of the tested soilbags. From the results of the pull test on the model slope, the equivalent coefficient of friction of the interlayer soilbags is calculated to be approximately 0.82, which is the ratio of half the maximum pulling force (the pulled soilbags are interlayered between the upper and the lower layers of soilbags) to the overburden load. In the model slope, the gap arrangement is somewhat similar to B_3 in Fig. 12(a). The small value of the equivalent coefficient of friction in the model slope may be attributed to the weak interlocking effect compared with B_3.

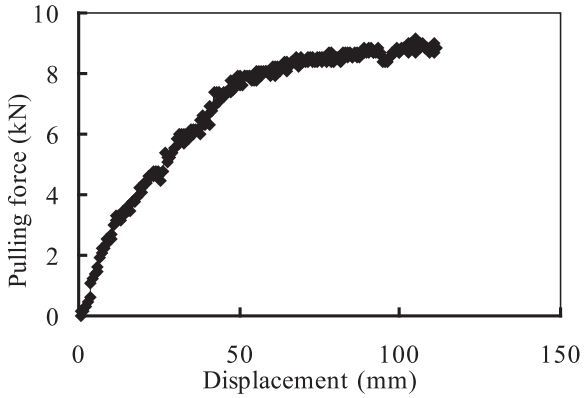

Fig. 15. Evolution of pulling force during test on model slope of soilbags

Stability Analysis for Slope Reinforced with Soilbags

As stated previously, the soilbags filled with expansive soil have high strength and can restrict the swelling deformation of the expansive soil inside. The assembly of these soilbags has a high permeability to prevent a great change of the water content in the expansive soil and a relatively high interlayer friction to maintain its stability. The assembly of these soilbags arranged on an expansive soil slope can also act as an overburden on the underlying expansive soil. As shown in Fig. 7, the swelling deformation of the expansive soil decreases with the increase in the pressure applied on the soil; that is, the overburden pressure has the effect of restricting the swelling deformation. In this section, the stability of a channel slope in the SNWTP is analyzed by taking the overburden of the soilbag assembly into account.

Fig. 16(a) shows a typical profile of the channel slope treated with soilbags in the SNWTP. The surface lining is covered through the whole profile, and the reinforcement layer is extended to the bottom of the channel. For the underlying expansive soil, it is possible to slide through the assembly of soilbags in two ways: one is along an interlayer contact plane (horizontal plane), as denoted by the slip of ACD, and the other is across the soilbags, as denoted by the slip of $A_1C_1D_1$. Because an expansive soil slope often fails in the shallow (Ng et al. 2003; Bao and Ng 2000) and the interlayer between the soilbags is a relatively weak plane, the possibility of sliding along ACD is considered to be higher than that along $A_1C_1D_1$.

To evaluate the stability of the reinforced slope, the forces acting on the assembly of the soilbags and on the underlying expansive soil are analyzed separately, as shown in Fig. 16(b). The equilibrium of the forces acting on the assembly of soilbags gives

J. Aerosp. Eng. 2013.26:657-666.

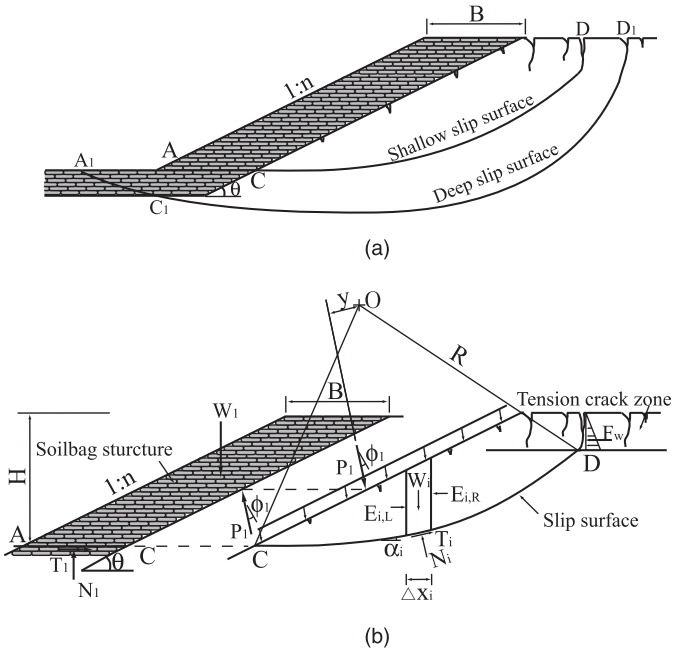

Fig. 16. Typical profile of channel slope treated with soilbags: (a) possible sliding surfaces; (b) forces acting on assembly of soilbags and underlying slope

$$T_1 = P_1 \sin(\theta - \phi_1)$$
$$N_1 = W_1 - P_1 \cos(\theta - \phi_1) \tag{8}$$

where N_1 and T_1 = normal force and horizontal resistant force on base of soilbag assembly, respectively; W_1 = weight of assembly of soilbags; P_1 = resultant force of soilbag assembly on underlying soil slope; ϕ_1 = friction angle mobilized in contact surface of soilbag structure and expansive soil; and θ = slope angle.

Taking F_s as the factor of safety of the reinforced slope and μ as the coefficient of the interlayer friction between the soilbags yields

$$T_1 = \frac{\mu \cdot N_1}{F_s} \tag{9}$$

Combining Eqs. (8) and (9) gives the value of P_1 as follows:

$$P_1 = \frac{\mu \cdot W_1}{F_s \cdot \sin(\theta - \phi_1) + \mu \cdot \cos(\theta - \phi_1)} \tag{10}$$

Assuming that the force of P_1 is uniformly applied on the surface of the underlying soil slope, then the uniform pressure p, which is regarded as the overburden pressure caused by the assembly of soilbags, is calculated as

$$p = P_1 \sin\theta / H \tag{11}$$

where H = height of assembly of soilbags that may slide along with underlying soil.

The factor of safety F_s may be calculated using the Fellenius method (Venkatramaiah 1997). Usually, there exist some tensile cracks in the ground surface of expansive soils caused by repeated wetting and drying for a long time. It is assumed that the slip surface through the tensile crack zone is vertical and that the shear strength of the expansive soil in this zone is zero. By taking the overburden pressure p and the tensile crack zone into account, the factor of safety F_s is calculated as

$$F_s = \frac{\sum\left\{c_i \cdot l_i + \left[(W_i + q_i \Delta x_i)\cos\alpha_i + p\Delta x_i \frac{\cos(\theta - \phi_1 - \alpha_i)}{\cos\theta}\right]\tan\phi_i\right\}}{\sum[(W_i + q_i \Delta x_i)\sin\alpha_i] + \frac{M_p}{R} - \frac{P_1 \cdot y}{R}} \tag{12}$$

where c_i and ϕ_i = apparent shear strength parameters of expansive soil; and M_p = moment of water pressure in crack zone. The other symbols are illustrated in Fig. 16(b).

Based on the experimental study by Liu et al. (2010), the apparent shear strength parameters of the NY expansive soil are related to the overburden pressure applied on the soil, and may be expressed as

$$c = 23.4 + \frac{\sigma_n}{0.5465 + 0.0163\sigma_n}$$
$$\phi = 9.62 + 0.0024\sigma_n \tag{13}$$

where σ_n = overburden pressure. In the calculation using Eq. (12), σ_n is the normal stress on the base of the slices.

As an example, a real channel expansive soil slope in the SNWTP, which has a height of 15 m and a gradient of 1:1.5, has been analyzed using Eq. (12). The slope is reinforced by the soilbags with a horizontal width of 3 m. The shear strength of the expansive soil as expressed by Eq. (13) was used in the calculation, and ϕ_1 and μ were taken as 16° and 0.84, respectively. To simplify the analysis, the crack zone was ignored, and thus both the values of M_p and q_i in Eq. (12) were assumed to be zero. Fig. 17 shows the slope analyzed and the contours of the factors of safety of the slope calculated. The minimum factor of safety F_s of the slope with and without the reinforcement of soilbags is calculated to be 1.46 and 1.23, respectively. The effectiveness of the reinforcement with the soilbags is illustrated clearly in this example.

Conclusions

In this study, a method of reinforcing the expansive soil slope in the SNWTP with soilbags is proposed. The reinforcement principle is presented, and the effectiveness of the soilbags is verified through a number of laboratory tests and the stability analysis for a reinforced expansive soil slope. The main conclusions may be included as follows:

- The soilbag filled with expansive soils has a high compression strength because an additional cohesion is produced by the tensile force T along the bag, which is developed after the extension of the bag perimeter (for an expansive soilbag, the extension of the

J. Aerosp. Eng. 2013.26:657-666.

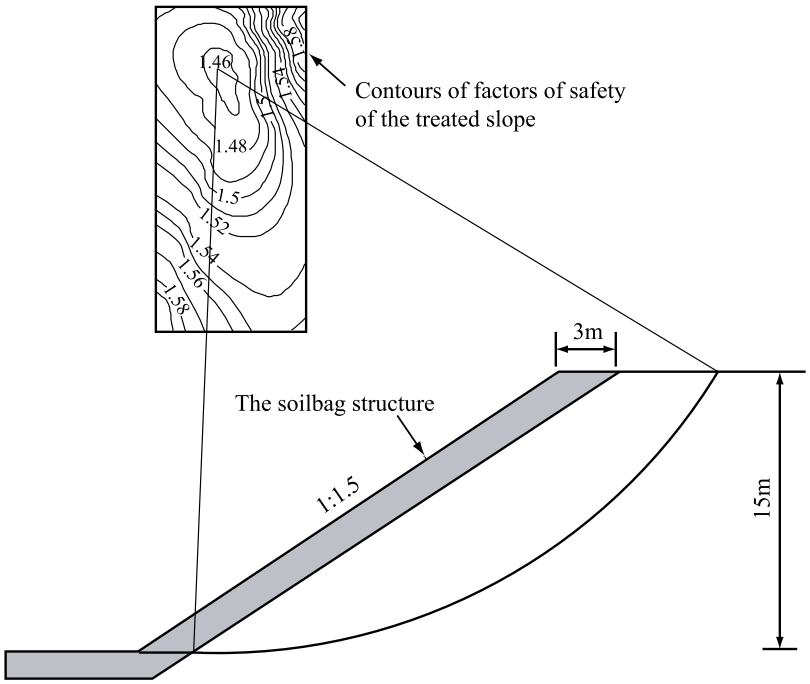

Fig. 17. Example of expansive soil slope treated by soilbags

bag perimeter is caused not only by the actions of external forces, but also by the swelling deformation of expansive soils);

- The swelling deformation and the swelling pressure of the expansive soilbag are smaller than those of the expansive soil at the same initial conditions;
- The permeability coefficient of the soilbag assembly ranges from 10^{-5} to 10^{-6} m/s, which makes it possible to minimize the variation of the water contents not only in the soilbag assembly (the reinforced layer), but also in the underlying expansive soils, probably caused by the rainfall or the change of the underground water;
- The assembly of soilbags has a relatively high equivalent coefficient of interlayer friction because of the interlocking effect in the gaps between soilbags; and
- The assembly of soilbags on the expansive soil slope acts as an overburden: for the calculated example, the increment of the factor of safety F_s is approximately 18.7%, illustrating the effectiveness of the proposed method.

Acknowledgments

This work was supported by Key Projects in the National Science and Technology Pillar Program during the 11th 5-year Plan Period of PR China (Grant No. 2006 BAB04A10). It was also a part of work in the project funded by the Priority Academic Program Development of Jiangsu Higher Education Institutions (PAPD).

References

Al-Mhaidib, A. I. (1998). "Swelling behaviour of expansive shales from the middle region of Saudi Arabia." *Geotech. Geol. Eng.*, 16(4), 291–307.

Bao, C. G., and Ng, C. W. W. (2000). "Some thoughts and studies on the prediction of slope stability in expansive soils." *Proc., 1st Asian Conf. on Unsaturated Soils*, Balkema, Rotterdam, Netherlands, 15–32.

Chen, F. H. (1988). *Foundation on expansive soils*, Elsevier, Amsterdam, Netherlands.

Day, R. W. (2000). *Geotechnical engineer's portable handbook*, McGraw Hill, New York.

Desai, I. D., and Oza, B. N. (1997). "Influence of anhydrous calcium chloride on shear strength of expansive soils." *Proc., 1st Int. Symp. on Expansive Soils*, HBTI, Kanpur, India, 4-1–4-5.

Katti, R. K. (1979). "Search for solutions to problems in black cotton soils." *Indian Geotech. J.*, 9(1), 1–80.

Liu, S. H., Wang, Y. S., Zhu, K. S., and Wu, J. (2010). "Experimental study on strength characteristics of Nanyang expansive soil under loading and its application." *J. Hydraul. Eng.*, 41(3), 361–367 (in Chinese).

Lu, N., and Likos, W. J. (2004). *Unsaturated soil mechanics*, Wiley, Hoboken, NJ.

Matsuoka, H., and Liu, S. H. (2003). "New earth reinforcement method by soilbags (DONOW)." *Soils Found.*, 43(6), 173–188.

Matsuoka, H., and Liu, S. H. (2005). *A new earth reinforcement method using soilbags*, Balkema, Rotterdam, Netherlands.

Ministry of Water Resources. (1999). "Specification of soil test." *SL237-1999*, Beijing (in Chinese).

Nakagawa, Y., Chen, G. L., Tatsui, T., and Chida, S. (2008). "Verification of vibration reduction characteristics with soilbag structure." *Proc., 4th Asian Regional Conf. on Geosynthetics*, Springer Verlag, Shanghai, China, 603–608.

Ng, C. W. W., Zhan, L. T., Bao, C. G., Fredlund, D. G., and Gong, B. W. (2003). "Performance of an unsaturated expansive soil slope subjected to artificial rainfall infiltration." *Geotechnique*, 53(2), 143–157.

Satyanarayana, B. (1966). "Swelling pressure and related mechanical properties of black cotton soils." Ph.D. thesis, Indian Institute of Science, Bangalore, Karnataka, India.

Sharma, R. S., Phanikumar, B. R., and Rao, B. V. (2008). "Engineering behavior of a remolded expansive clay blended with lime, calcium chloride, and rice-husk ash." *J. Mater. Civ. Eng.*, 20(8), 509–515.

Tatsuoka, F., and Tateyama, T. (1997). "Geosynthetic-reinforced soil retaining walls as important permanent structures." *Geosynth. Int.*, 4(2), 81–136.

Venkatramaiah, C. (1997). *Geotechnical engineering*, 3rd Ed., New Age International, New Delhi, India, 327.

Zhan, L. T., Ng, C. W. W., and Fredlund, D. G. (2007). "Field study of rainfall infiltration into a grassed unsaturated expansive soil slope." *Can. Geotech. J.*, 44(4), 392–408.